Journal Européen des Systèmes Automatisés
Vol. 59, No. 1, January, 2026, pp. 125-132
Journal homepage: http://iieta.org/journals/jesa

Reflex-Based Adaptive Locomotion for Biped Robots Using Piezoelectric Sensing on Slippery Terrain

Anas Yassin*, Yarub Alazzawi

Department of Mechatronics Engineering, Al-Khwarizmi College of Engineering, University of Baghdad, Baghdad 10001, Iraq

Corresponding Author Email: Anas.Yassin1602a@kecbu.uobaghdad.edu.iq

https://doi.org/10.18280/jesa.590112

Received: 6 November 2025
Revised: 11 January 2026
Accepted: 20 January 2026
Available online: 31 January 2026

Keywords:
bipedal robot, robot locomotion, piezo-sensor, slippery ground, stability

ABSTRACT

Bipedal robots face many issues with stability through walking on slippery environments, and traction can lead to falls with potential mechanical damage when reduced. These challenges are identified as dangerous conditions in real time due to the complexity of slip behavior and the limited processing capabilities of embedded systems. To address these challenges, a reflexive-based control strategy is employed with piezoelectric sensors within the support polygon of the robot foot to classify the surface type under the robot foot by measuring force response. Surfaces separated and signals filtered using an Exponential Moving Average (EMA) filter for normal (rough) and slippery surfaces. The results show that on standard conditions of terrains (rough), robots maintain balancing with shorter stance duration (≈ 0.2 s) and high joint speed (≈ 125◦/s). In contrast, through walking on a slippery environment, the reflex controller increases the stance duration (≈ 0.38 s) and decreases the speed (≈ 53◦/s) to enhance balancing. These results demonstrate that a lightweight reflex-based control system can adapt to slip conditions effectively. Furthermore, it offers an economical and simple method to improve the safety of this type of robot in unstructured environments.

1. INTRODUCTION

Humanoid robot locomotion is an essential function, and it is a common difficult problem in robotics. Despite wheeled robots, bipedal robots depend on dynamic balancing and precise coordination of their legs to stand in balance while walking. When the robot faces an unpredictable environment, such as slick ground, it falls down and loses stability. Falls cause mechanical damage in the robot structure, not only reducing the operational efficiency [1-3], which makes stability during movement a key challenge in the current study.

The main challenge in this research is represented by the difficult stability of biped robots when facing a sudden environment with a frictional surface. Furthermore, slip ground is represented as a common gap in legged robot society because it is classified as highly non-linear time-varying behavior and is hard to model. These issues lead to unpredictable responses in ground reaction forces, which make stability control in real-time a major challenge. In addition, the response of controllers for environments like this type must give fast correction actions to prevent falls through locomotion. In practice, the absence of a computationally efficient and robust control framework that can adapt gait parameters dynamically through walking remains a limitation. On the other hand, many model-based locomotion control studies assume predictable environment contact. Stability fails with assumptions like these when slip occurs because the interaction between the robot and this type of terrain becomes strongly and highly non-linear [4, 5].

Legged robots are not fixed to a surface, which makes motion control a significant challenge to avoid falling and stay stable. Stability is important because it determines whether the robot is capable of performing the task required efficiently or not. Over the past few decades, progress has been made in legged robotics systems, which has led to major advances in control and stability research. This development is particularly essential in biped robots, especially these systems designed to mimic or replicate humans in their environments [6-9].

Humanoid robots differ from each other significantly in control and mechanical structures, and many researchers are aiming to produce human-like behavior and smoothness. This development involves the integration of sensors and natural behaviors. A stronger psychological tendency between humans and humanoid robots, making a significant interaction between human perception and robot engineering design [10, 11]. Falling robots not only affect the tasks but also may create a risk for nearby people. For this reason, designing a mechanism that can adapt between different types of environments to enable real-time adjustment is a practical and scientific challenge. Bipedal gait generation has grown in recent years, especially when these robots become integrated into the daily life environment. Natural human-inspired locomotion has been achieved by many researchers, which enhances the robot interaction quality and realism [12].

A wide range of techniques has been developed for stability improvement in a bipedal robot. Techniques such as ZMP-based, which is a conventional control to enhance stability, typically focus on the accuracy of the dynamical model [13,

14]. In addition, these methods will perform with predictable terrains, but they struggle with unexpected slip surfaces, their assumption of stability, and fixed contact between the ground and the robot's foot.

Many approaches introduce the modeling of slipping. Mihalec et al. [15] combined the Fractional Whole Body Operational Space (FWBOS) with a linear inverted pendulum of two masses by a hierarchical control framework to control slipping. While their method is promising, it is limited to movement in the sagittal plane and does not take into account lateral slippage or rotational effects, which are essential for the robot's movement in a realistic environment. In a related study, Ghorbani et al. [16] developed a simplified model of centrifugal dynamics that adjusts the step length to prevent slippage; however, this technique limits the natural motion of the robot and fails to account for differences in angular momentum. Franco et al. [17] introduced a biology-inspired approach for the NAO robot by integrating predictive gait with balance control. This control layer improves stability depending on computational machine learning, which poses a challenge to deploy on a robot. Brandao et al. [18] investigated motion on low-friction surfaces that lead to tipping and mechanical damage. The proposed strategy of gait planning depends on the Required Coefficient of Friction (RCOF) that modifies parameters such as duration, step timing, CoM, and step length to decrease the risk of slipping. This framework was implemented in a simulation on a 48 DOF humanoid robot. It depends on heavy friction estimation and computational cost, which reduces robustness.

Despite these advances in locomotion control, two challenges are common and unsolved yet. Firstly, slippage controllers depend on complex modeling, which makes them hard to work on low-power controllers and increases the computational cost. Secondly, many methods don't have the ability to generate responses compared with humans' responses, which are essential to avoid sudden slipping through locomotion. To address these challenges, this research introduces a reflex-based, lightweight, and adaptive control framework to maintain the stability of locomotion under different conditions of friction. This motivation is essential to introduce the proposed reflex control architecture.

Reflex control is inspired by biological neuromuscular reflexes observed in humans and animals, where rapid corrective actions are generated at the spinal level in response to sensory feedback, such as muscle stretch or ground contact forces [19]. Unlike high-level voluntary motor planning, these reflex pathways operate with minimal latency and do not rely on explicit predictive models of the system dynamics. Compared to traditional model-based predictive control (MPC), reflex-based strategies have demonstrated improved robustness and computational efficiency in highly dynamic and uncertain environments [20].

The novelty in this research is represented in the integration of piezoelectric sensing with an adaptive reflexive control architecture that can respond fast, avoid slippage in real time, and adjust corrections for joint parameters through walking. With this framework, there is no need to implement additional sensors or computational processing. Unlike conventional systems with fixed parameters without correction, self-adjusting parameters enable continuous adaptation and serve the simple implementation on controllers. This design is a lightweight and cost-effective solution to respond to slipping in bipedal robots' locomotion.

This paper is separated into many sections, as follows: Section 1 covers the research background with the main challenge and motivation. Section 2 explains the overall control mechanism, system design, and hardware setup. Section 3 shows and analyzes the results and discussion. Section 4 highlights the limitations of this study. Finally, Section 5 includes the conclusions and future work.

2. METHODS

2.1 Design

Because this study focuses on robotic movement and not human participants, the "population" is defined as the set of surfaces and walking experiences that the robot encounters, as follows:

•Normal (rough) surface
•Slippery surface

The bipedal robot completed multiple walking trials on both surfaces, producing sensor data that comprised the dataset for analysis. A purposeful sampling approach was used to ensure that the selected surfaces represented two extreme categories: stable, high-friction terrain (rough) and unstable, low-friction terrain (slip surface). This contrasting condition allowed for an accurate assessment of the system's ability to avoid terrains. For each surface type, three walking sessions were conducted to capture variability and ensure the reproducibility of results. The slippery surface condition was created by applying a thin, uniform layer of commercial sunflower cooking oil on rigid ground surface. The normal (non-slippery) condition used the wood surface in a dry state. Sunflower oil was selected due to its stable lubrication properties and availability. The effective coefficient of friction is significantly reduced compared to dry surfaces. The same surface and lubrication conditions were used consistently across all experiments to ensure repeatability.

Piezoelectric sensors were used to detect foot-ground contact and surface conditions during walking. Sensor data were acquired at an effective sampling frequency of approximately 200 Hz, determined by the sensor acquisition loop timing. Raw analog signals were processed online to enable rapid reflex responses, as shown in Figure 1.

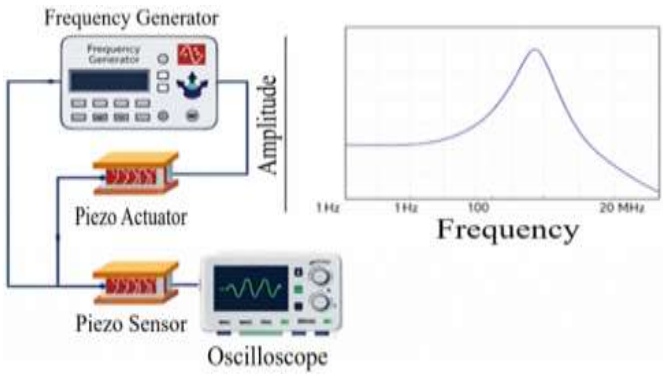

Figure 1. Frequency response test for piezoelectric transducer

A 6-DoF robot with two legs, each consisting of three joints: hip (forward/backward), knee (backward bend), and ankle (side-to-side swing), Figure 2. Two discs of piezoelectric sensors are mounted on the robot's foot sole for signal detection and surface classification, as shown in Figure 3. An

Arduino Uno board was used for real-time signal acquisition and motor control. Power was supplied by two 3.7 V lithium batteries in series, regulated through a DC-DC step-down converter to provide 5 V. A protection board was included for safe charging, as shown in Figure 4.

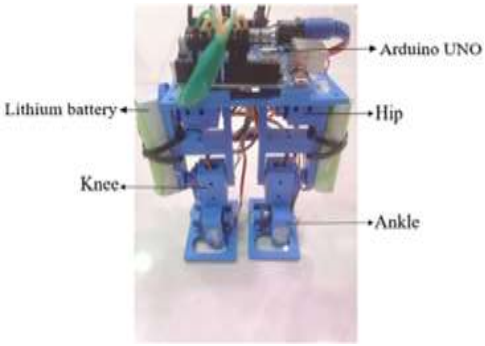

Figure 2. Biped robot prototype

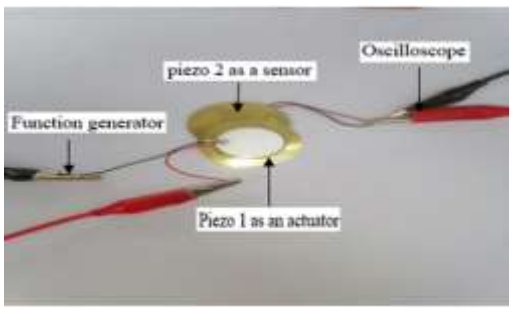

Figure 3. Frequency response testing setup for piezo elements

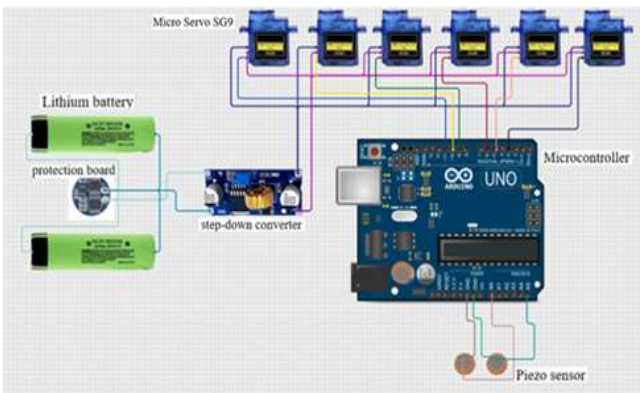

Figure 4. Circuit design of control electronics

Sensor calibration was performed in situ during walking experiments. Raw piezoelectric data were collected while the robot walked on normal (non-slipping) and slippery surfaces. From these data, statistical features including peak amplitude, and signal standard deviation were extracted to characterize surface conditions. Baseline reference values were obtained from nominal walking trials and used to define thresholds distinguishing slipping from non-slipping states.

2.2 Data collection and signal processing

Data collection was performed using piezoelectric sensors embedded in the support polygon of the robot's feet, as shown in Figure 5. These sensors generated voltage signals in response to ground reaction forces through walking on two environments, as shown in Figure 6. The signals were read as analog inputs through an Arduino Uno microcontroller, which also controlled the six servo motors responsible for the robot's leg movements.

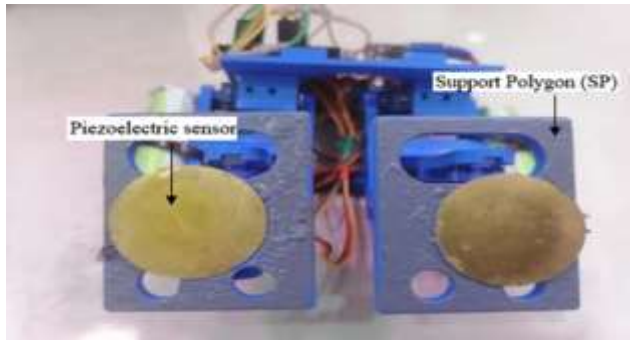

Figure 5. Two piezo elements embedded with robot feet

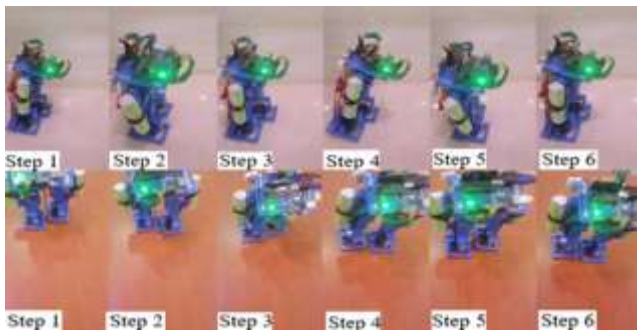

Figure 6. Bipedal robot walking on different surfaces

The data were transmitted serially from the Arduino to a Python script running on a computer, as shown in Figure 7. The Python script stored the data for subsequent analysis. Each walking session produced data that included peak amplitude, standard deviation, rise time, and other parameters relevant to surface classification.

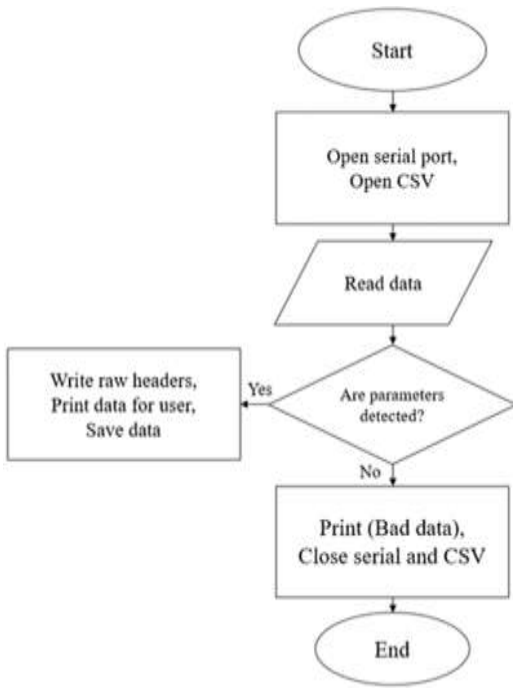

Figure 7. Obtaining data flowchart

To reduce measurement noise while preserving fast transient responses, an Exponential Moving Average (EMA) filter was applied to the sensor signals with a smoothing factor of α = 0.12. This filtering strategy provided a balance between noise attenuation and low-latency feedback, which is essential for reflex-based control.

Each piezo signal was sampled as an analogue value:

$$V_{piezo}(t) = \text{analog (pin)} \quad (1)$$

Assume each foot have a piezo sensor:

F_L (t), F_R (t): instantaneous analog reading, normalized force:

$$f_{L,R}(t) = \frac{F_{L,R}(t) - F_{min}}{F_{max} - F_{min}} \quad (2)$$

where,

$f_{L,R}$: Normalized piezo force (dimensionless, range [0, 1]).

$F_{L,R}(t)$: Instantaneous raw piezo sensor readings (ADC value).

F_{min}: Minimum calibration value when the foot is unloaded (no contact with ground).

F_{max}: Maximum calibration value under full contact or (maximum load).

When $f_{L,R}$ (t) = F_{min} then $f_{L,R}$ (t) = 0 (no contact with surface).

When $f_{L,R}$ (t) = F_{max} then $f_{L,R}$ (t) = 1 (full contact with surface).

Intermediate value 0 < $f_{L,R}$ (t) < 1 represent partial contact or transient state during stepping.

Features extracted as sum of readings:

$$S = \sum_{i=0}^{N-1} F_i \quad (3)$$

where,

S: the total contact energy or accumulated piezo force signals over the entire contact period.

F_i: the instantaneous piezo sensor readings at the sample.

N: total number of samples recorded during the contact.

A large sum indicates a strong impact or firm contact (hard or rough surface). And a small sum suggests weak impact or energy loss typical of slip or soft ground. The average forces applied by the foot during contact while walking. It gives the baseline pressure level of the foot on the ground.

$$\bar{F} = \frac{S}{N} \quad (4)$$

where,

$\bar{F}$: Average contact pressure.

High mean: Stable support, firm surfaces.

Low mean: Incomplete support or early slip occurs.

The standard deviation represents the variation or fluctuation in the contact pressure:

$$\sigma = \sqrt{\frac{1}{N}\sum_{i=0}^{N-1}(F_i - \bar{F})^2} \quad (5)$$

where,

σ: Forces variability.

High σ: Large variation in foot-ground interaction (noise, vibration, slipping).

Low σ: Stable, uniform pressure (steady stance on solid surface).

In Reflex Control:

A high σ might indicate instability or vibrations caused by rough (normal) surfaces.

A very low σ with a low mean may indicate loss of traction or foot slipping.

The total time the foot stays in contact with the surface represents contact durations as follows:

$$T_{contact} = t_{end} - t_{start} \quad (6)$$

where,

$T_{contact}$: Time of stance phase to adjust gait cycles timing.

Short $T_{contact}$: Faster step, possibly due to slip or run motion.

Long $T_{contact}$: Steady stance, possibly during stand or firm walking.

2.3 Reflex detection logic

Reflex is triggered if sudden changes in stance foot forces are detected:

$$Slip_{L,R} = \begin{cases} 1, & if\ \sigma < \sigma_{thresh.}\ or\ S > S_{thresh.} \\ 0, & Otherwise \end{cases}$$

where,

$\sigma_{thresh.}$: Normal (rough surface) threshold.

$S_{thresh.}$: Slippery surface threshold.

When a piezo-based surface detection algorithm determines a slip event, the robot must react rapidly by modifying its joint angles to restore balance or traction. These modifications are expressed as joint angle increments (Δθ) for the hip, knee, and ankle joints.

(a) Hip adjustment (swing leg)

$$\Delta\theta_{hip} = K_{hip}.Slip_{stance} \quad (7)$$

When a slip is detected during the stance phase, the robot changes the hip swing amplitude to shorten or lengthen the steps. The gain determines how strongly the hip responds to a slip. If the stance foot slips backward (forward walking), the swing hip should move forward faster to regain support. This helps stabilize the center of mass (CoM) over the support foot.

(b) Knee adjustment

$$\Delta\theta_{knee} = K_{knee}.Slip_{stance} \quad (8)$$

The knee flexion is increased or decreased depending on slip intensities. K_{knee} is the reflex gain for knee responses. A slipping foot may require more knee flexion to lower the center of mass and increase frictional forces. This mimics human reflex actions; we instinctively bend our knees when we feel a slip.

(c) Ankle adjustment (stance leg)

$$\Delta\theta_{ankle} = K_{ankle}.Slip_{stance}.\text{Direction} \quad (9)$$

The ankle adjusts to shift body weight opposite to the slip directions. Direction = +1 for left slip, −1 for right slip. If the right foot slips backward, the ankle on that leg dorsiflexes (toe up) while the opposite foot pushes down (plantar flexion) to redistribute support. This is equivalent to a corrective torque to restore balance.

$Slip_{stance}$ is a measure of the slip magnitude derived from piezo sensor features:

$$Slip_{stance}=\alpha_1.(\text{STDDEV-6})+\alpha_2.–(\text{S-S}_{th}) \quad (10)$$

where,

6: measured standard deviation (sensors stability).

S: sum of readings (total contact energy).

α_1, α_2: tuning coefficients.

This combine information about how much contact variations or energy loss occurred representing slip intensity.

Now, the reflex response (Δθ) is added to the robot's baseline joint commands. The sum produces a new commanded joint angle sent to the servo motor.

$$\Theta_{joint}(t)=\Theta_{baseline}(t)+\Delta\Theta_{reflex}(t)$$

where,

$$\Delta\Theta_{reflex}(t) = \begin{cases}\Delta\Theta_{hip}, \Delta\Theta_{knee}, \Delta\Theta_{ankle}, if\ slip\ detected \\ 0, otherwise\end{cases}$$

$\Theta_{baseline}(t)$: normal locomotion joint trajectory (from gait pattern generator).

$\Delta\Theta_{reflex}(t)$: rapid corrective adjustments (reflex output).

This mimics the spinal reflex loop in humans:

Piezo sensor: equivalent to mechanoreceptors in the foot.

Slip detection: equivalent to spinal interneuron processing.

Δθ output: equivalent to muscle activation reflexes that adjust limb stiffness and posture.

To ensure validity, experiments were conducted under controlled conditions with consistent surface preparation for both normal and slippery trials. The slippery surface was always created using oil.

Reliability was maintained by repeating each walking experiment three times for both surfaces. Data from repeated trials were averaged, as shown in Figure 8, and the mean error was calculated to reduce the influence of outliers. The use of an EMA filter further enhanced reliability by reducing high-frequency noise in the sensor readings without altering the main signal trends. Figure 9 represents the control architecture diagram for the system.

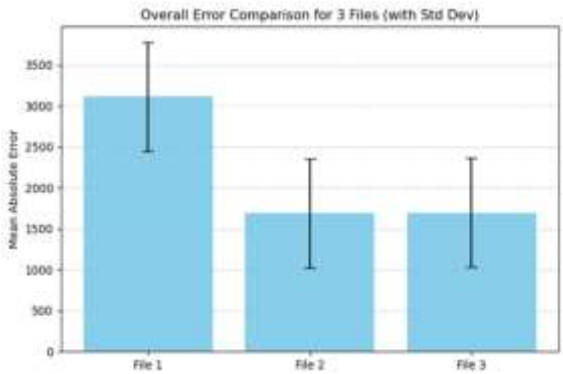

Figure 8. Mean absolute error for a slippery surface

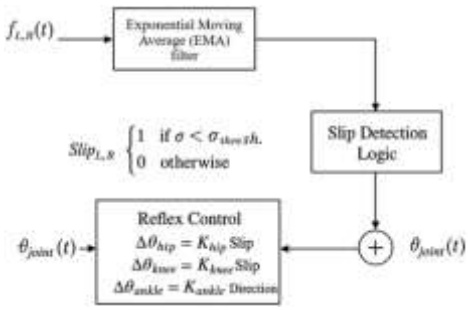

Figure 9. Control architecture diagram

3. RESULTS AND DISCUSSION

The experiments generated data from piezoelectric sensors embedded in the feet of the 6-DoF biped robot as it walked across two types of surfaces:

•Normal (rough) surface.

•Slippery surface.

Each condition was tested in three separate walking trials, and data were recorded through the Arduino Uno microcontroller and transmitted to a Python script. Raw piezo signals were passed through an EMA filter to reduce noise and smooth fluctuations. Six numerical parameters were extracted from each walking trial, including standard deviation, sum of values, peak amplitude, rise time, and related features. On non-slip surfaces, the robot assumes a natural walking posture in terms of speed and stride length; conversely, on slippery surfaces, the robot reduces speed and takes smaller steps.

During slipping, the robot walks without falling and maintains stability. The variations in the Center of Mass (CoM) are shown in Figure 10 on the X-axis during walking. The behavior of the Center of Mass shows that there is periodic oscillation over the gait cycle, indicating that the body shifts side to side to stay stable, depending on ankle control. In addition, the CoM trajectory stays inside stability limits. This demonstrates that the controller maintains balance effectively even through repeated movement cycles. The transient at the start of moving indicates robot phase stabilization before achieving steady-state movement. The result shows that the reflex combination and transitions of smooth servo maintained the stability successfully during locomotion.

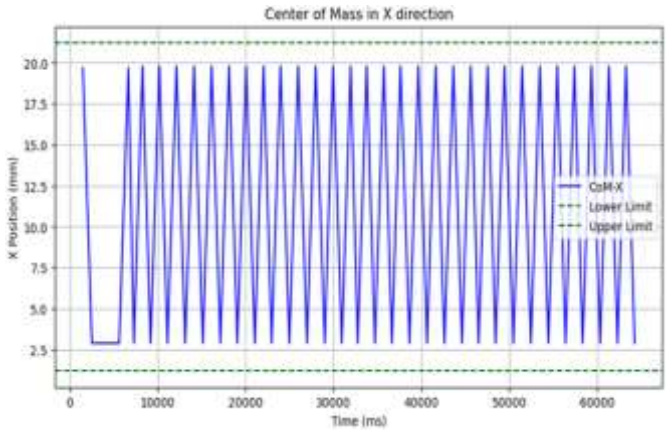

Figure 10. Behavior of Center of Mass (CoM) trajectories in x-axis during forward locomotion

The reflex unit effectively mitigates mild slippage. A 60% reduction indicates that the reflex corrections (ankle/hip/knee)

are working quickly enough to counteract early slippage. However, when slip amplitude exceeds ~0.85, the foot is already sliding significantly, making full recovery more difficult. This behavior aligns with biological reflex response in human walking, small slips are corrected reflexively, while large slips often require whole body compensation, as shown in Figure 11. The Figure compares the measured slip amplitude for each gait cycle with the corresponding slip reduction percentage achieved by the reflex controller. The result shows that most walking cycles show zero slip, indicating stable ground contact and consistent foot placement. When slip occurs (between 0.35–0.95 slip units), the reflex controller consistently reduces slip by ~60%, except when the foot loses traction completely. In cycles with 100% slip reduction, the terrain impact was minimal, and the controller successfully prevented the initiation of slipping.

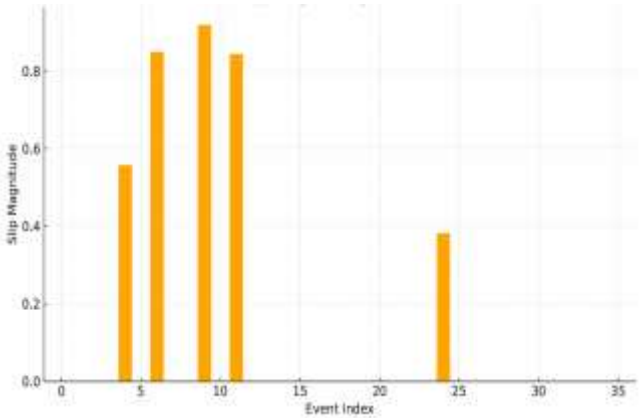

Figure 11. Slip magnitude per event (step)

The joint-level corrective response is proportional to slip severity. This demonstrates that the reflex controller incorporates a graded correction strategy similar to neuromuscular reflexes, where a small slip triggers a small correction and a large slip triggers full multi-joint reflex action, as shown in Figure 12. This figure demonstrates how the reflex joint correction (combined hip, knee, and ankle) scales with slip amplitude. Reflex corrections activate only when (slip > 0), indicating clean threshold-based activation. High-slip event (≥ 0.8) triggers the largest correction magnitude, often involving (ankle + knee + hip) compensation. Moderate slips (~0.35–0.55) typically result in ankle-only or (ankle + hip) corrections. For a cycle without slip, the correction magnitude remains zero, confirming that the reflex system does not introduce unnecessary movement.

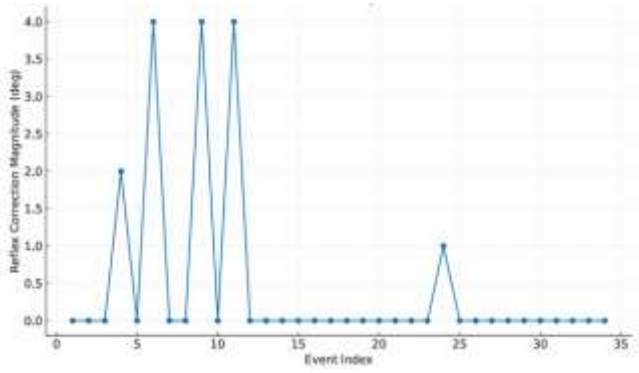

Figure 12. Reflex correction per event (step) response

The relationship between slip magnitude and the reflex correction magnitude generated by the robot's joint-level reflexive controller is shown in Figure 13. The data shows a clear positive correlation. As the slip magnitude increases, the reflex system progressively takes larger corrective actions. Readings of slip close to (0.35–0.55) elicit a moderate response (1–2 units), while consistently high slip values exceeding 0.80 result in strong reversal corrections (4 units). This trend confirms that the reversal algorithm determines its corrective effort according to the disturbance severity rather than applying a fixed reaction. At zero point, the slip is equal to zero, which indicates a rough surface or non-slipping cycle. Activation lack indicates that there are no false corrections in reflex activations, as previous findings prove that threshold control effectively prevents unintended reactions during steady walking. Table 1 shows the results of 34 walking steps in real time.

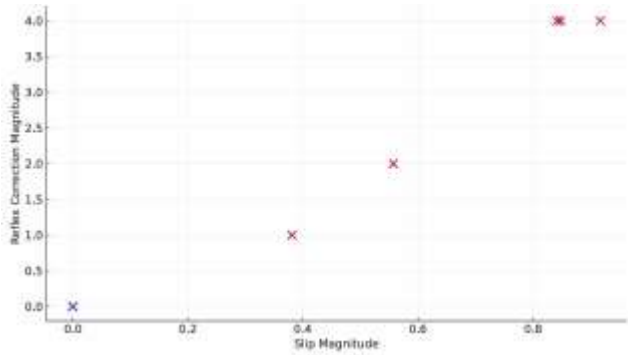

Figure 13. The size of the reflexive correction for each event (step)

Table 1. Real time adaption data recorded during locomotion

Metric	Result	Interpretation
False positives	0% after per-foot thresholding	Calibration successful
Reaction time	0–5 m s	Near-instantaneous reflex activation
Recovery success rate	100%	No falls or instability after detection
Computational load	Minimal	Suitable for real-time embedded implementation

The results showed that the piezoelectric sensor can distinguish between slippery and non-slip surfaces. The EMA filter effectively filters the signals of the piezoelectric sensor and enhances the detection. The robot maintains high velocity and short stance duration in case of normal (rough) surface (125°/s, 0.2 s). In contrast, when the slip was detected, the robot maintained an extended stance and decreased angular velocity (53°/s, 0.38 s), mimicking human behavior through slowing motion to stay stable. Table 2 contains the walking parameters of the robot joints through each surface.

Table 2. Robot joints parameters during adaptation between surfaces

Surface class	Rough Surface	Slippery Surface
Step duration	0.2 s (0.4 s gait cycle)	0.38 s (0.76s gait cycle)
Angular velocity	125 deg. Per sec.	53 deg. Per sec.

The results expand the literature and are compared with previous studies on adaptive locomotion. ZMP traditional controller [4] gives effective behavior on structured terrains (flat ground) but fails with the slip condition because it assumes the foot contact with the ground is fixed. Approaches in references [7, 8] introduce a model-based framework with a constrained dynamical model for an accurate and flexible system. In reference [9], the researchers employed learning to predict slipping, which makes the method heavy and computationally demanding for an embedded system. Similarly, Jenelten et al. [4] decreased slip risk by using RCOF-based methods, but this assumption depends on high computation requirements and friction estimation, which limits adaptability to slip changes. In contrast, reflexive gait adaptation in real time was achieved in this research with a piezoelectric sensor and filtering, as shown in Table 3.

The results highlight the bio-inspired reflex architecture's effectiveness. From mounting a piezoelectric sensor within the robot's foot to motor response, the system shows the ability to stabilize and rapidly adapt, mimicking humans. This work contributes to the expanding research body that supports lightweight, feedback-based control strategies for biped locomotion in an unstructured environment.

Table 3. Comparison of previous studies with present study on biped locomotion

Approach	Method	Strength	Limitation
Traditionl ZMP-based control [4]	Trajectory planning to keep ZMP within support polygon.	Effective on flat, predictable ground; well-established.	Assumes fixed ground contact; fails under slips.
Mihalec et al. [15]	Hierarchical model (FWBOS + TMLIP) with slip handling.	Explicit slip-aware planning; hierarchical design.	Limited to sagittal plane; requires detailed friction modeling.
Ghorbani et al. [16]	Centroidal dynamics with step-length adjustment.	Reduces modeling error; ensures gait periodicity.	Restricts CoM flexibility; ignores angular momentum.
Franco et al. [17]	Bio-inspired control with proactive + reactive layers; ML-based friction prediction.	Improves stability; human-like adaptation.	Requires machine learning inference; heavy computation unsuitable for embedded hardware.
Brandao et al. [18]	Anticipatory gait planning using Required Coefficient of Friction (RCOF).	Reduces slippage risk by adjusting gait timing, COM trajectory, and support phases; validated on 48-DOF KOBIAN.	Relies on accurate friction estimation; computationally demanding; limited adaptability to sudden slips.
Present research (Reflex + Piezo)	Reflex controller with piezo sensing + EMA filtering.	Real-time, low-cost, bio-inspired reflex adaptation; works on microcontrollers.	Tested on limited surfaces and simplified robot prototype.

4. LIMITATIONS

Mechanical limits and inherent noise play an important role in limiting the performance of a system, but several other practical problems also profoundly condition its operation. Control latency, i.e. the time delay between signal processing and actuation, can cause a loss of reactivity for reflex-based controllers and, in turn, provoke instability under fast perturbations. In addition, sensor delays and processing times lead to a difference between the measured state and the actual state of a coupling system that requires prompt re-adjustment. Multidirectional slip on the contact surface, especially on irregular or low-friction terrains, may affect foot placement and stability of locomotion at least for horizontal compensation. These may need to be taken into account in future models, which try to quantify how often a system will fail under real conditions of use.

5. CONCLUSIONS

In this work, we show that reflexive control with embedded piezoelectric sensors can significantly improve the perturbations of a biped on rough and slippery floors. Surface types are classified with force measurements and signals using an EMA filter processed by the controller to modify gait parameters in real-time. On rough treated surfaces the robot keeps balance with a small stance duration of 0.225 s and high joint speed of ≈ 126°/s, whilst on slippery ones the reflexive responses lead to a longer stance duration of 0.37 s and reduced joint speed below 53°/s, providing certainly for a stable situation over falling one. These results quantitatively verify that the proposed lightweight reflex-based framework can quickly adjust to different traction conditions, introducing a simple and cost-effective way to enhance the safety and robustness of legged robots in unstructured terrain.

Future work will include developing and testing the system with a wide range of surfaces, such as ice and wet tiles. In addition, enhance and develop the mechanical design of the robot platform to mimic human ankle design, swing forward and backward, not only side to side, to cover the limitations of the system design.

REFERENCES

[1] Kwon, O., Park, J.H. (2002). Reflex control of bipedal locomotion on a slippery surface. Advanced Robotics, 16(8): 721-734. https://doi.org/10.1163/15685530260425710

[2] Tazaki, Y., Murooka, M. (2020). A survey of motion planning techniques for humanoid robots. Advanced Robotics, 34(21-22): 1370-1379. https://doi.org/10.1080/01691864.2020.1803128

[3] Wang, H., Huang, W. (2025). Gait generation and motion implementation of humanoid robots based on hierarchical whole-body control. Electronics, 14(23): 4714. https://doi.org/10.3390/electronics14234714

[4] Jenelten, F., Hwangbo, J., Tresoldi, F., Bellicoso, C.D., Hutter, M. (2019). Dynamic locomotion on slippery

ground. IEEE Robotics and Automation Letters, 4(4): 4170-4176. https://doi.org/10.1109/LRA.2019.2931284

[5] Takabayashi, Y., Ishihara, K., Yoshioka, M., Liang, H., Liu, C., Zhu, C. (2017). Frictional constraints on the sole of a biped robot when slipping. In 2017 IEEE/RSJ International Conference on Intelligent Robots and Systems (IROS), Vancouver, BC, Canada, pp. 5011-5016. https://doi.org/10.1109/IROS.2017.8206384

[6] Brecelj, T., Petrič, T. (2022). Zero moment line—Universal stability parameter for multi-contact systems in three dimensions. Sensors, 22(15): 5656. https://doi.org/10.3390/s22155656

[7] Mikolajczyk, T., Mikołajewska, E., Al-Shuka, H.F.N., Malinowski, T., et al. (2022). Recent advances in bipedal walking robots: Review of gait, drive, sensors and control systems. Sensors, 22(12): 4440. https://doi.org/10.3390/s22124440

[8] Tayal, M., Kolathaya, S. (2023). Safe legged locomotion using collision cone control barrier functions (C3BFs). arXiv preprint arXiv:2309.01898. https://doi.org/10.48550/arXiv.2309.01898

[9] Heng, S., Zang, X., Song, C., Chen, B., Zhang, Y., Zhu, Y., Zhao, J. (2024). Balance and walking control for biped robot based on divergent component of motion and contact force optimization. Mathematics, 12(14): 2188. https://doi.org/10.3390/math12142188

[10] Rahman, S.M., Ikeura, R. (2012). International symposium on robotics and intelligent sensors 2012 (IRIS 2012) estimating and validating relationships between actual and perceived weights for lifting objects with a power assist robot: The psychophysical approach. Procedia Engineering, 41: 685-693. https://doi.org/10.1016/j.proeng.2012.07.230

[11] Sun, W., Chen, L., Su, Y., Cao, B., Liu, Y., Xie, Z. (2025). Learning humanoid locomotion with world model reconstruction. arXiv preprint arXiv:2502.16230. https://doi.org/10.48550/arXiv.2502.16230

[12] Ferreira, J.P., Franco, G., Coimbra, A.P., Crisóstomo, M. (2020). Human-like gait adaptation to slippery surfaces for the NAO robot wearing instrumented shoes. International Journal of Humanoid Robotics, 17(3): 2050007. https://doi.org/10.1142/S0219843620500073

[13] Xi, A., Chen, C. (2020). Stability control of a biped robot on a dynamic platform based on hybrid reinforcement learning. Sensors, 20(16): 4468. https://doi.org/10.3390/s20164468

[14] Al-Tameemi, I., Amanuel, O. (2025). Bipedal robots: A systematic review of dynamical models, balance control strategies, and locomotion methods. Journal of Robotics and Control, 6(3): 1240-1254.

[15] Mihalec, M., Han, F., Yi, J. (2022). Integrated inverted pendulum and whole-body control design for bipedal robot with foot slip. IFAC-PapersOnLine, 55(37): 376-381. https://doi.org/10.1016/j.ifacol.2022.11.212

[16] Ghorbani, E., Karimpour, H., Pasandi, V., Keshmiri, M. (2022). Footstep adjustment for biped push recovery on slippery surfaces. Multibody System Dynamics, 56(3): 189-219. https://doi.org/10.1007/s11044-022-09842-z

[17] Franco, G., Coimbra, A., Crisóstomo, M., Ferreira, J. (2021). The NAO robot in slippery scenarios: A strategy. Journal of Information Systems Engineering and Management, 6(1): em0133. https://doi.org/10.29333/jisem/9572

[18] Brandao, M., Hashimoto, K., Santos-Victor, J., Takanishi, A. (2014). Gait planning for biped locomotion on slippery terrain. In 2014 IEEE-RAS International Conference on Humanoid Robots, Madrid, Spain, pp. 303-308.

[19] Bunz, E.K., Haeufle, D.F.B., Schmitt, S., Geijtenbeek, T. (2025). A simple network of proprioceptive reflexes can produce a variety of bipedal gaits. BioRxiv Preprint. https://doi.org/10.1101/2025.02.05.636668

[20] Grube, M., Wieck, J.C., Seifried, R. (2022). Comparison of modern control methods for soft robots. Sensors, 22(23): 9464. https://doi.org/10.3390/s22239464